

See discussions, stats, and author profiles for this publication at: <https://www.researchgate.net/publication/231667244>

# Structure Sensitivity for Forward and Reverse Water–Gas Shift Reactions on Copper Surfaces: A DFT Study

ARTICLE *in* JOURNAL OF PHYSICAL CHEMISTRY LETTERS · OCTOBER 2010

Impact Factor: 7.46 · DOI: 10.1021/jz101150w

---

CITATIONS

37

---

READS

21

2 AUTHORS, INCLUDING:



Gui-Chang Wang

Nankai University

78 PUBLICATIONS 810 CITATIONS

SEE PROFILE

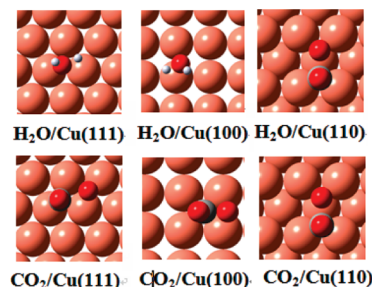
# Structure Sensitivity for Forward and Reverse Water-Gas Shift Reactions on Copper Surfaces: A DFT Study

Gui-Chang Wang<sup>\*,†,§</sup> and Junji Nakamura<sup>\*,†</sup>

<sup>†</sup>Department of Chemistry, Nankai University, Tianjin, 300071, P. R. China, <sup>§</sup>College of Chemistry and Environmental Science, Shanxi Datong University, Datong, 037009, Shanxi Province, P. R. China, and <sup>\*</sup>Institute of Materials Science, University of Tsukuba, 1-1-1 Tennoudai, Tsukuba, Ibaraki, 305-8573 Japan

**ABSTRACT** The DFT-GGA calculations have clearly reproduced the experimentally observed structure-sensitivity of forward and reverse water-gas shift reactions on Cu(111), Cu(100), and Cu(110) assuming the “redox mechanism”. The reason for the structure-sensitivity has also been explored by the transition-state structure analysis and the metal d-band center analysis. It is concluded that the difference in virtual adsorption energy of atomic oxygen or other strongly adsorbed species at the transition state is essential to account for the structure-sensitive reactions.

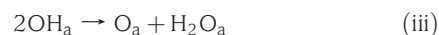
**SECTION** Surfaces, Interfaces, Catalysis



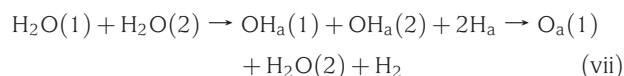
Catalytic activities of solid surfaces are sometimes significantly different depending on the surface structure. The structure sensitivity of heterogeneous catalysis is one of the most important problems in understanding the active sites. Many catalytic systems have been classified into the structure sensitive reaction by surface science experiments using single crystal surfaces, which have been carried out since the 1970s. However, it has been still under speculation on the atomic level why and how the structure sensitivity appears because of shortage on the quantitative kinetic information such as the detailed catalytic mechanism, the rate determining step, and the kinetics of elementary steps. Theoretical analyses for the transition state (TS) of the surface reaction and the electronic structure are required to clarify the structure sensitive features appeared on different surface orientations. Density functional theory (DFT) study combined with kinetic data obtained by surface science experiments is suitable to solve the problem of the structure sensitivity.

The catalytic water-gas shift (WGS) reaction ( $\text{CO} + \text{H}_2\text{O} \rightarrow \text{CO}_2 + \text{H}_2$ ) as well as the reverse water-gas shift (RWGS) reaction ( $\text{CO}_2 + \text{H}_2 \rightarrow \text{CO} + \text{H}_2\text{O}$ ) on Cu surfaces are well known to be a typical structure-sensitive reaction, in which the reaction rate of WGS on Cu(110) is higher than that on Cu(111).<sup>1,2</sup> However, the reason why both forward and reverse WGS reactions are structure-sensitive is not clear, although some empirical theoretical methods have been used to explore such phenomena.<sup>3,4</sup> The reaction mechanism and the rate-determining step of WGS and RWGS reactions on Cu have been well-studied by using traditional catalytic research techniques and surface science approaches. Two different mechanisms, that is, “redox mechanism”<sup>1,2,5–7</sup> and “carboxyl intermediate mechanism”,<sup>8–10</sup> are possible for the forward WGS reaction on copper surfaces, where the latter mechanism has been newly proposed by DFT. The mechanism of the reverse WGS reaction has not been discussed by DFT. In experiments, the following “redox mechanism” has been

proposed for both forward and reverse WGS reactions on the Cu(110) surface.<sup>1,2,5–7</sup>



It should be noted that adsorbed oxygen in the redox mechanism is assumed to be formed by reaction iii, that is, recombination of  $\text{OH}_a$ , instead of direct dissociation of  $\text{OH}_a$  into  $\text{O}_a$  and  $\text{H}_a$  because reaction iii is a well known reaction taking place on Cu easily at ca. 270 K. In the literature, the mechanism has been called a “water-catalyzed mechanism”,<sup>1</sup> in which water molecules are classified into reactant and catalyst, that is,  $\text{H}_2\text{O}(1)$  and  $\text{H}_2\text{O}(2)$  in the following equation.



A water molecule,  $\text{H}_2\text{O}(1)$ , dissociates into  $\text{OH}_a(1)$  and then  $\text{O}_a(1)$ , subsequently. The other water molecule,  $\text{H}_2\text{O}(2)$ , once dissociates into  $\text{OH}_a(2)$ , which does not further dissociate into surface oxygen but comes back to  $\text{H}_2\text{O}(2)$  after abstraction of proton from  $\text{OH}_a(1)$ . That is,  $\text{H}_2\text{O}(2)$  or  $\text{OH}_a(2)$  play a role as a

**Received Date:** August 14, 2010

**Accepted Date:** September 22, 2010

**Published on Web Date:** October 04, 2010

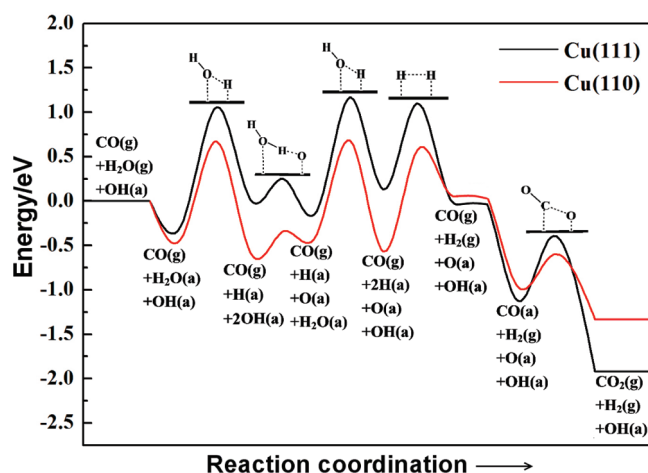


**Figure 1.** Calculated potential diagram by DFT for the redox mechanism of water-gas shift reaction on Cu(111) and Cu(110).

catalyst for the conversion of  $\text{OH}_a$  (1) to  $\text{O}_a$  (1). It is thus possible to call it a “ $\text{OH}_a$  catalyzed mechanism”.

Although the mechanism of the WGS reaction has been studied by DFT,<sup>8–10</sup> the structure sensitivity has not been studied for both forward and reverse WGS reactions so far. In this work, we use the DFT-GGA method with the periodic slab model to study the reaction mechanism of WGS reaction as well as reverse WGS reaction and attempt to explore the nature of the structure sensitivity by analyzing the TS of  $\text{H}_2\text{O}$  or  $\text{CO}_2$  dissociation.

In this study, the assumed redox mechanism composed of reactions i–vi was first elucidated by the DFT calculation to see whether the DFT study can be applicable to reproduce the experimental results of the WGS reaction on Cu surfaces. Figure 1 shows the potential diagram for the redox mechanism of the WGS reaction on Cu(111) and Cu(110), obtained by DFT-GGA calculation. The “ $\text{OH}_a$ -catalyzed mechanism” is involved in this diagram, as shown by  $\text{OH}_a$  added to reactants and products in Figure 1. The calculated potential diagram for Cu(110) is very similar to that obtained by experiments.<sup>1</sup> That is, the dissociation of adsorbed  $\text{H}_2\text{O}$  reveals the highest barrier for the WGS reaction, whereas the dissociation of  $\text{CO}_2$  reveals the highest barrier for the RWGS reaction. It has been accepted that the rate-limiting steps of the WGS and the RWGS reactions are  $\text{H}_2\text{O}$  dissociation and  $\text{CO}_2$  dissociation, respectively, based on the measurements of dissociation probabilities of  $\text{H}_2\text{O}$  or  $\text{CO}_2$  on Cu as well as pressure dependence of  $\text{H}_2\text{O}$  or  $\text{CO}_2$  on the reaction rates of the WGS or the RWGS reactions. The other steps, that is, eqs i, iii, iv, and vi, have not so high barriers, which is also consistent with the experimental results on Cu(111) and Cu(110), as discussed in the literature.<sup>1,2,5,6,11–14</sup>

Now, let us look at the detailed energetics for the elementary steps of the WGS reaction on Cu. In Table 1, the DFT-GGA results of activation barriers for the elementary steps of the forward ( $E_{a,f}$ ) and the reverse ( $E_{a,r}$ ) WGS reactions on Cu(111), Cu(100), and Cu(110) are summarized to compare with experimental data. First, the “water-catalyzed mechanism” was examined by the DFT-GGA calculation. It is confirmed that

**Table 1.** Activation Energies of Forward ( $E_{a,f}$ ) and Reverse ( $E_{a,r}$ ) Elementary Steps Involved in the WGS Reaction on Cu(*hkl*) Surfaces<sup>a</sup>

	Cu(111)		Cu(100)		Cu(110)	
	$E_{a,f}$	$E_{a,r}$	$E_{a,f}$	$E_{a,r}$	$E_{a,f}$	$E_{a,r}$
$\text{H}_2\text{O}_a = \text{OH}_a + \text{H}_a$	1.28	1.04	1.23	1.10	1.05	1.25
$\text{OH}_a = \text{O}_a + \text{H}_a$	1.51	0.85	1.60	0.88	1.43	0.57
$2\text{OH}_a = \text{H}_2\text{O}_a + \text{O}_a$	0.23	0.36	0.10	0.40	0.24	0.03
$2\text{H}_a = \text{H}_{2,a}$	0.97	1.08	0.62	0.30	1.10	0.56
$\text{CO}_a + \text{O}_a = \text{CO}_{2,a}$	0.71	1.51	0.63	1.26	0.34	0.71

<sup>a</sup> Energy unit in electronvolts.

the activation energy for the step of  $\text{OH}_a \rightarrow \text{O}_a + \text{H}_a$  (1.43 to 1.60 eV) is much higher than that of  $2\text{OH}_a \rightarrow \text{H}_2\text{O} + \text{O}_a$  (0.10 to 0.24 eV), as shown in Table 1, supporting that the adsorbed oxygen atom is easily formed by the associative reaction of  $2\text{OH}_a \rightarrow \text{H}_2\text{O} + \text{O}_a$  rather than the direct dissociation of  $\text{OH}_a$ , as suggested in the experiments.<sup>1</sup> This means that the DFT results support the “ $\text{OH}_a$ -catalyzed mechanism”. Mavrikakis et al.<sup>9</sup> have also reported that the OH disproportionation in the “water-catalyzed mechanism” is a facile step for producing atomic oxygen on Cu(111). Their calculated barriers for  $\text{OH}_a \rightarrow \text{O}_a + \text{H}_a$  and  $2\text{OH}_a \rightarrow \text{H}_2\text{O}_a + \text{O}_a$  on Cu(111) are 1.76 and 0.23 eV, respectively, which are comparable to our data, 1.51 and 0.23 eV, respectively. However, they have considered that the  $\text{OH}_a$  disproportionation is not involved in the WGS reaction mechanism because they have proposed the carboxyl mechanism of  $\text{CO}_a + \text{OH}_a \rightarrow \text{COOH}_a \rightarrow \text{CO}_2 + \text{H}_a$ .<sup>9</sup>

The next important point is the structure sensitivity of the WGS and the RWGS reactions on Cu, which should be originated from the structure sensitivity of the rate-limiting step of the  $\text{H}_2\text{O}$  dissociation and the  $\text{CO}_2$  dissociation, respectively. Here one can easily find that the calculated activation energies of the  $\text{H}_2\text{O}_a$  dissociation decrease in the order of (111), (100), and (110), with barriers of 1.28, 1.23, and 1.05 eV, respectively. The large difference in the dissociation barrier among these three surfaces implies that the WGS reaction is a structure-sensitive reaction. The calculated activation energies of the  $\text{H}_2\text{O}_a$  dissociation are close to the experimental results of 1.23 eV on Cu(111)<sup>11</sup> and 0.87 eV on Cu(110).<sup>12,13</sup> The calculated barrier for  $\text{H}_2\text{O}_a$  dissociation on Cu(111) here, 1.28 eV, is close to that calculated by Mavrikakis et al., 1.36 eV.<sup>9</sup> Mavrikakis et al.<sup>9</sup> have reported that the activation energy of  $\text{H}_2\text{O}$  on Cu(211) is identical to that on Cu(111), suggesting that the specific bond-breaking event may be quasi-structure-insensitive.

As for the RWGS reaction, the calculated activation energy of the  $\text{CO}_2$  dissociation on Cu(111) (1.51 eV) is much higher, as compared with those of Cu(100) (1.26 eV) and Cu(110) (0.71 eV). These agree with the experimentally measured apparent activation energy of the  $\text{CO}_2$  dissociation, 0.95 eV on Cu(100)<sup>15</sup> and 0.63 eV on Cu(110),<sup>9</sup> if one assumes a small adsorption energy of  $\text{CO}_2$  at 0.1 to 0.3 eV.<sup>16</sup> Both calculated and measured barriers for the  $\text{CO}_2$  dissociation are further comparable to the apparent activation energy of the RWGS reaction, 1.40 eV on poly-Cu (mainly Cu(111) at 5 atm),<sup>14</sup> 1.34 eV on Cu(100) at 18 atm,<sup>17</sup> and 0.78 eV at 0.01 to 2.6 atm,<sup>13</sup>

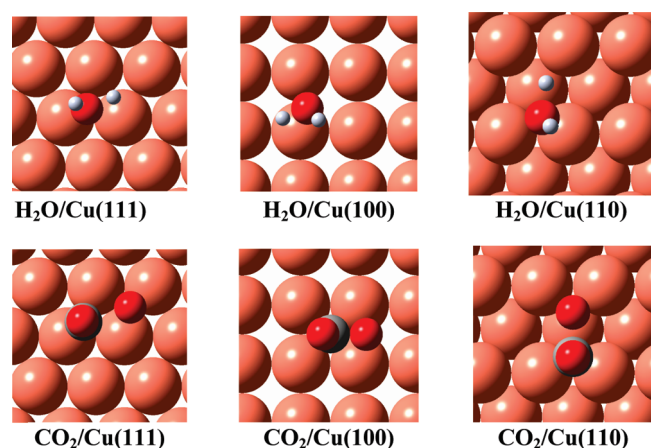


**Figure 2.** Transition state of H<sub>2</sub>O and CO<sub>2</sub> dissociations on Cu(111), Cu(100), and Cu(110).

0.81 eV at 5 atm,<sup>2</sup> and 1.17 eV at 18 atm<sup>17</sup> on Cu(110). Additionally, the larger barrier for Cu(111) has been reported in the previous DFT results, 1.69<sup>9</sup> and 1.93 eV.<sup>18</sup> The significant difference in the barrier of the CO<sub>2</sub> dissociation among these Cu surfaces well explains the structure sensitivity of the RWGS reaction. Note that the dissociation barrier calculated here is for the formation process of adsorbed O and adsorbed CO from adsorbed CO<sub>2</sub>, not from gas-phase CO<sub>2</sub>. In the experiment, however, apparent activation energy of CO<sub>2</sub> dissociation corresponds to the change in potential energy for the process from gas-phase CO<sub>2</sub> to adsorbed O and adsorbed CO because CO<sub>2</sub> adsorption energy is too small to allow measurement of the dissociation rate of adsorbed CO<sub>2</sub>.

The good agreements in the activation barriers between the experiments and the DFT calculation allow us to apply the DFT calculation for examining more detailed mechanism of H<sub>2</sub>O and CO<sub>2</sub> dissociations. The TSs of the H<sub>2</sub>O dissociation and the CO<sub>2</sub> dissociations on Cu(111), Cu(100), and Cu(110) have thus been examined, as shown in Figure 2. The local orientation of H<sub>2</sub>O and CO<sub>2</sub> to the substrate registry seems to be apparently different depending on the Cu surface plane. However, a common point is there. The adsorbed H<sub>2</sub>O or CO<sub>2</sub> molecule seems to have been already dissociated at TS. The structure parameters, that is, bond length, of TS are summarized in Table 2. It turns out that the bond length of H and O (1.23 to 1.59 Å) in H<sub>2</sub>O and that of C and O (1.58 to 2.23 Å) in CO<sub>2</sub> are much larger than the O–H bond length (0.96 Å) of a gas-phase H<sub>2</sub>O molecule and C=O bond length (1.16 Å) in a gas-phase CO<sub>2</sub> molecule, respectively. This means the bond breaking at TS for both the H<sub>2</sub>O dissociation and the CO<sub>2</sub> dissociation. The other bond lengths of O–H (0.99 Å) of OH<sub>a</sub> and C–O (1.18 to 1.21 Å) of CO<sub>a</sub> are close to those of gas-phase H<sub>2</sub>O and CO<sub>2</sub> molecules, respectively. The TS structures for the dissociations of H<sub>2</sub>O<sub>a</sub> → H<sub>a</sub> + OH<sub>a</sub> and CO<sub>2,a</sub> → CO<sub>a</sub> + O<sub>a</sub> on copper are thus more like products (CO<sub>a</sub> and O<sub>a</sub>) rather than reactant (CO<sub>2,a</sub>), which is so-called “late barrier”.

In the case of “late barrier” for H<sub>2</sub>O dissociation, the O–H bond in H<sub>2</sub>O is broken at TS. On the basis of the relative positions of atoms (hydrogen and oxygen) over Cu atoms at TS, virtual adsorption energies of OH<sub>a</sub> and H<sub>a</sub> at TS as well as

**Table 2.** Structure Parameter of Transition States for H<sub>2</sub>O and CO<sub>2</sub> Dissociations on Copper (Bond Length in angstroms)

	<i>d</i> <sub>C–M</sub>	<i>d</i> <sub>O–M</sub>	<i>d</i> <sub>C–O1</sub>	<i>d</i> <sub>C–O2</sub>	<i>d</i> <sub>O–H1</sub>	<i>d</i> <sub>O–H2</sub>
H <sub>2</sub> O on Cu(100)		2.04			0.99	1.23
H <sub>2</sub> O on Cu(110)		1.96			0.99	1.59
H <sub>2</sub> O on Cu(111)		2.05			0.99	1.34
CO <sub>2</sub> on Cu(100)	2.38	1.88	1.21	1.58		
CO <sub>2</sub> on Cu(110)	2.11	1.93	1.19	1.97		
CO <sub>2</sub> on Cu(111)	2.01	1.90	1.18	2.23		

**Table 3.** Virtual Adsorption Energies and Interaction Energies of Adsorbed Species at TS for CO<sub>2</sub> Dissociation (Left Half) and H<sub>2</sub>O Dissociation (Right Half)<sup>a</sup>

	<i>E</i> <sub>Oa</sub>	<i>E</i> <sub>COa</sub>	<i>E</i> <sub>Oa/COa</sub>	<i>E</i> <sub>Ha</sub>	<i>E</i> <sub>OHa</sub>	<i>E</i> <sub>Ha/OHa</sub>
Cu(111)	−4.02	−0.63	0.18	−2.06	−2.44	0.39
Cu(100)	−4.02	−0.67	−0.01	−2.01	−2.56	0.23
Cu(110)	−4.32	−0.80	−0.09	−1.86	−2.90	0.15

<sup>a</sup>Energy is estimated based on the atomic position at TS (electronvolts).

interaction energy between OH<sub>a</sub> and H<sub>a</sub> can be estimated by the DFT calculation. The total energy of TS, *E*<sub>TS</sub>, and the energy of Cu substrate, *E*<sub>Cu</sub>, are divided into the virtual adsorption energies of OH<sub>a</sub> and H<sub>a</sub> and the interaction energy between H<sub>a</sub> and OH<sub>a</sub>, *E*<sub>Ha/OHa</sub>, as follows

$$E_{\text{TS}} + E_{\text{Cu}} = E_{\text{Ha}} + E_{\text{OHa}} + E_{\text{Ha/OHa}} \quad (\text{viii})$$

Table 3 summarizes the virtual adsorption energy of H<sub>a</sub> and OH<sub>a</sub> at TS of H<sub>2</sub>O dissociation as well as the virtual adsorption energy of O<sub>a</sub> and CO<sub>a</sub> at TS of CO<sub>2</sub> dissociation. The virtual adsorption energy of OH<sub>a</sub> decreases in the order of Cu(110), Cu(100), and Cu(111). On the contrary, the virtual adsorption energy of H<sub>a</sub> decreases slightly in the order of Cu(111), Cu(100), and Cu(110). The larger adsorption energy leads to lower barrier at TS. That is, the stronger bonding between OH<sub>a</sub> and Cu results in reduction of activation barrier of H<sub>2</sub>O dissociation. The order of surface planes in the activation energy of H<sub>2</sub>O dissociation, Cu(111) > Cu(100) > Cu(110), can thus be explained by the adsorption energy of OH<sub>a</sub>, Cu(111) < Cu(100) < Cu(110). The major origin of structure sensitivity for dissociation of H<sub>2</sub>O on Cu is thus ascribed to the interaction between OH and Cu atoms at TS. The same argument can be applied to the dissociation of CO<sub>2</sub> on Cu. As shown in Table 3, the virtual adsorption energy of O<sub>a</sub> at TS is much larger than that of CO<sub>a</sub>. The larger adsorption energy of O<sub>a</sub> leads to lower activation energy of CO<sub>2</sub> dissociation. Again, the reason for the lower activation barrier of CO<sub>2</sub> dissociation on Cu(110) is due to the higher adsorption energy of O<sub>a</sub> on Cu(110) at TS. It may be a general trend that the structure sensitivity of dissociation reactions with late barrier is due to difference in the adsorption energy of species interacting with surface most strongly at TS. In both cases of H<sub>2</sub>O and CO<sub>2</sub> dissociations, the interaction of oxygen atom and copper atom determines the structure sensitivity instead of hydrogen or carbon atoms. Moreover, it can be seen from Table 3 that the interaction energies between two separated



**Table 4.** Adsorption Energy of Species Related to WGS Reaction (electronvolts)<sup>a</sup>

	Cu(111)	Cu(100)	Cu(110)
H <sub>2</sub> O	0.22	0.25	0.38
H	2.73	2.38	2.61
OH	3.26	3.51	3.62
CO	1.14	0.83	1.03
O	5.30	5.77	5.45

<sup>a</sup> Data are shown for the most stable adsorption sites.

species at TS, H–OH and O–CO, are also correlated with the activation barrier order, that is, the larger attraction energy, the lower activation barrier.

Because it is widely known that the d-band center can be used to predict surface reactivity,<sup>19</sup> the structure sensitivity of H<sub>2</sub>O dissociation and the CO<sub>2</sub> dissociation were tried to be elucidated by the d-band center of Cu(111), Cu(100), and Cu(110). In the present study, the d-band center based on the local density of state (LDOS) diagrams were estimated to be –3.00, –2.80, and –2.45 eV for (111), (100), and (110), respectively. The order is consistent with the trend of the activity for dissociation of H<sub>2</sub>O and CO<sub>2</sub>; that is to say, the closer to the Fermi level for the d-band center, the easier for the dissociation of H<sub>2</sub>O as well as CO<sub>2</sub>. Note that one cannot always use the d-band center as criteria to predict the structure sensitivity of metal surfaces. Table 4 shows the adsorption energies of species related to the WGS reaction on Cu(111), Cu(100), and Cu(110), in which the adsorption energies at the most stable sites are shown. It is clear that the d-band center criteria cannot apply to predict the order of the Cu surfaces in terms of the largest adsorption energy. For example, the order in the adsorption energy of oxygen on Cu(111), Cu(100), and Cu(110) cannot be explained by the d-band center, where the four-fold hollow site of Cu(100) is the most stable for the adsorption of atomic oxygen. In general, the adsorption energy of atom is dependent on the adsorption site significantly in the case of an identical kind of metal. The d-band center thus may be used to predict a trend in the adsorption energy or the structure sensitivity if the adsorption site is identical on the same kind of metal. As shown in Figure 2, the positions of OH<sub>a</sub> of H<sub>2</sub>O as well as O<sub>a</sub> of CO<sub>2</sub> in the TS structure seem to be all bridge sites. This may be the reason why the d-band center of Cu can be used for the prediction of trend in the activation barriers.

Finally, the proposed picture of the CO<sub>2</sub> dissociation mechanism by the DFT study is compared with the successful DFT results explaining the nature of activation barrier for CO oxidation (CO<sub>a</sub> + O<sub>a</sub> → CO<sub>2</sub>) on Pt(111) by Hu et al.<sup>20,21</sup> The CO oxidation is the reverse process of the CO<sub>2</sub> dissociation. They have reported that the predominant energy to overcome the activation barrier of the CO oxidation is ascribed to the breaking energy of strong oxygen–metal bond. At the TS, oxygen moves from the most stable three-fold hollow site to bridge site, at which CO<sub>a</sub> reacts with O<sub>a</sub>. The bridge site of oxygen at TS was also observed for CO<sub>2</sub> dissociation on Cu in this study, as shown in Figure 2. The results of both Hu et al. and us suggest that the atomic oxygen on the bridge site may

be very active like the oxygen at the TS of CO<sub>2</sub> dissociation or CO oxidation.

In summary, the structure-sensitivity of forward and RWGS reactions on Cu(111), Cu(100), and Cu(110) surfaces was studied by DFT-GGA calculations assuming the “redox mechanism”. The calculation reproduced the experimentally measured potential diagram, in which the dissociation of H<sub>2</sub>O is the rate-determining step for the forward WGS reaction, whereas the dissociation of CO<sub>2</sub> is that for the reverse WGS reaction. The activation energies for both dissociations of H<sub>2</sub>O and CO<sub>2</sub> decrease in the order of Cu(111) > Cu(100) > Cu(110). At the TS of the dissociations, O–H bond in H<sub>2</sub>O as well as C–O bond in CO<sub>2</sub> are broken, that is, “late barrier”, so that the activation energies for the dissociation of H<sub>2</sub>O and CO<sub>2</sub> are influenced significantly by the virtual adsorption energy of OH<sub>a</sub> and O<sub>a</sub> at TS, respectively. The difference in the virtual adsorption energy at TS is thus essential to account for the structure-sensitive characters.

## CALCULATION MODEL AND METHODS

All calculations are performed using the plane-wave DFT (VASP code).<sup>22,23</sup> The exchange-correlation energy and potential are described by generalized gradient approximation (PW91).<sup>24</sup> The electron-ion interaction is described by the projector-augmented wave (PAW) scheme,<sup>25,26</sup> and the electronic wave functions are expanded by plane waves up to a kinetic energy of 400 eV. A periodical four-layer slab is used with ~10 Å of vacuum region between slabs. The calculated models are chosen as the unit cells of 2 × 2 with the corresponding coverage of 1/4 ML. During the calculation, the first two layers and the adsorbed species were allowed to be relaxed. The surface Brillouin zone is sampled using a 4 × 4 × 1 Monkhorst–Pack mesh.<sup>27</sup> The minimization of the reaction pathways and the search of the TSs have been performed with the climbing-image nudged elastic band method (CI-NEB).<sup>28,29</sup>

## AUTHOR INFORMATION

### Corresponding Author:

\*To whom correspondence should be addressed. (G.-C.W.) E-mail: wangguichang@nankai.edu.cn. (J.N.) Tel/Fax: +81-29-853-5279. E-mail: nakamura@ims.tsukuba.ac.jp.

## REFERENCES

- (1) Nakamura, J.; Campbell, J. M.; Campbell, C. T. Kinetics and Mechanism of the Water-Gas Shift Reaction Catalysed by the Clean and Cs-promoted Cu(110) Surface: A Comparison with Cu(111). *J. Chem. Soc., Faraday Trans.* **1990**, *86*, 2725–2734.
- (2) Yoshihara, J.; Campbell, C. T. Methanol Synthesis and Reverse Water–Gas Shift Kinetics over Cu(110) Model Catalysts: Structural Sensitivity. *J. Catal.* **1996**, *161*, 776–782.
- (3) Wang, G. C.; Jiang, L.; Cai, Z. S.; Pan, Y. M.; Zhao, X. Z.; Huang, W.; Xie, K. C.; Li, Y. W.; Sun, Y. H.; Zhong, B. Structure Sensitivity of the Water-Gas-Shift Reaction on Cu(*hkl*) Surface: A Theoretical Study. *J. Phys. Chem. B* **2003**, *107*, 557–562.
- (4) Wang, G. C.; Jiang, L.; Pang, X. Y.; Cai, Z. S.; Pan, Y. M.; Zhao, X. Z.; Morikawa, Y.; Nakamura, J. A Theoretical Study of

- Surface-Structural Sensitivity of the Reverse Water-Gas Shift Reaction over Cu(*hkl*) Surfaces. *Surf. Sci.* **2003**, *543*, 118–130.
- (5) Ovesen, C. V.; Stoltze, P.; Nørskov, J. K.; Campbell, C. T. A Kinetic Model of the Water Gas Shift Reaction. *J. Catal.* **1992**, *134*, 445–468.
  - (6) Ovesen, C. V.; Clausen, B. S.; Hammershøi, B. S.; Steffensen, G.; Askgaard, T.; Chorkendorff, I.; Nørskov, J. K.; Rasmussen, P. B.; Stoltze, P.; Taylor, P. A Microkinetic Analysis of the Water-Gas Shift Reaction under Industrial Conditions. *J. Catal.* **1996**, *158*, 170–180.
  - (7) Shumacher, N.; Boisen, A.; Dahl, S.; Gokhale, A. A.; Kandoi, S.; Grabow, L. C.; Dumesic, J. A.; Mavrikakis, M.; Chorkendorff, I. Trends in Low-Temperature Water-Gas Shift Reactivity on Transition Metals. *J. Catal.* **2005**, *229*, 265–275.
  - (8) Liu, P.; Rodriguez, J. A. Water-Gas-Shift Reaction on Metal Nanoparticles and Surfaces. *J. Chem. Phys.* **2007**, *126*, 164705-1–164705-8.
  - (9) Gokhale, A. A.; Dumesic, J. A.; Mavrikakis, M. On the Mechanism of Low-Temperature Water Gas Shift Reaction on Copper. *J. Am. Chem. Soc.* **2008**, *130*, 1402–1414.
  - (10) Tang, Q.; Chen, Z.; He, X. A Theoretical Study of the Water Gas Shift Reaction Mechanism on Cu(111) Model System. *Surf. Sci.* **2009**, *603*, 2138–2144.
  - (11) Campbell, C. T.; Daube, K. A. A Surface Science Investigation of the Water-Gas Shift Reaction on Cu(111). *J. Catal.* **1987**, *104*, 109–119.
  - (12) Nakamura, J.; Rodriguez, J. A.; Campbell, C. T. Does CO<sub>2</sub> Dissociatively Adsorb on Cu Surfaces? *J. Phys. (Condensed Matter)* **1989**, *1*, SB149–SB160.
  - (13) Ernst, K. H.; Campbell, C. T.; Moretti, G. Kinetics of the Reverse Water-Gas Shift Reaction over Cu(110). *J. Catal.* **1992**, *134*, 66–74.
  - (14) Yoshihara, J.; Parker, S. C.; Schafer, A.; Campbell, C. T. Methanol Synthesis and Reverse Water-Gas Shift Kinetics over Clean Polycrystalline Copper. *Catal. Lett.* **1995**, *31*, 313–324.
  - (15) Rasmussen, P. B.; Taylor, P. A.; Chorkendorff, I. The Interaction of Carbon Dioxide with Cu(100). *Surf. Sci.* **1992**, *269/270*, 352–359.
  - (16) Chorkendorff, I.; Rasmussen, P. B.; Christoffersen, H.; Taylor, P. A. The Stabilization of Adsorbed Carbon Dioxide by Formate on Cu(100). *Surf. Sci.* **1993**, *287/288*, 208–211.
  - (17) Nakamura, I.; Fujitani, T.; Uchijima, T.; Nakamura, J. The Synthesis of Methanol and the Reverse Water-Gas Shift Reaction over Zn-Deposited Cu(100) and Cu(110) Surfaces: Comparison with Zn/Cu(111). *Surf. Sci.* **1998**, *400*, 387–400.
  - (18) Michaelides, A.; Liu, Z. P.; Zhang, C. J.; Alavi, A.; King, D. A.; Hu, P. Identification of General Linear Relationships Between Activation Energies and Enthalpy Changes for Dissociation Reactions at Surfaces. *J. Am. Chem. Soc.* **2003**, *125*, 3704–3705.
  - (19) Hammer, B.; Nørskov, J. K. Theoretical Surface Science and Catalysis-Calculations and Concepts. *Adv. Catal.* **2000**, *45*, 71–128.
  - (20) Alavi, A.; Hu, P.; Deutsch, T.; Silverstrelli, P. L.; Hutter, J. CO Oxidation on Pt(111): An *Ab Initio* Density Functional Theory Study. *Phys. Rev. Lett.* **1998**, *80*, 3650–3653.
  - (21) Gong, X. Q.; Liu, Z. P.; Ravel, R.; Hu, P. A Systematic Study of CO Oxidation on Metals and Metal Oxides: Density Functional Theory Calculations. *J. Am. Chem. Soc.* **2004**, *126*, 8–9.
  - (22) Kresse, G.; Hafner, J. *Ab Initio* Molecular-Dynamics Simulation of the Liquid-Metal–Amorphous-Semiconductor Transition in Germanium. *Phys. Rev. B* **1994**, *49*, 14251–14269.
  - (23) Kresse, G.; Furthmüller, J. Efficiency of *Ab-Initio* Total Energy Calculations for Metals and Semiconductors using a Plane-Wave Basis Set. *Comput. Mater. Sci.* **1996**, *6*, 15–50.
  - (24) Perdew, J. P.; Chevary, J. A.; Vosko, S. H.; Jackson, K. A.; Pederson, M. R.; Singh, D.; Fiolhais, C. Atoms, Molecules, Solids, and Surfaces: Applications of the Generalized Gradient Approximation for Exchange and Correlation. *Phys. Rev. B* **1992**, *46*, 6671–6687.
  - (25) Blöchl, P. E. Projector Augmented-Wave Method. *Phys. Rev. B* **1994**, *50*, 17953–17979.
  - (26) Kresse, G.; Joubert, D. From Ultrasoft Pseudopotentials to the Projector Augmented-Wave Method. *Phys. Rev. B* **1999**, *59*, 1758–1775.
  - (27) Monkhorst, H. J.; Pack, J. D. Special Points for Brillouin-Zone Integrations. *Phys. Rev. B* **1976**, *13*, 5188–5192.
  - (28) Henkelman, G.; Uberuaga, B. P.; Jónsson, H. A Climbing Image Nudged Elastic Band Method for Finding Saddle Points and Minimum Energy Paths. *J. Chem. Phys.* **2000**, *113*, 9901–9904.
  - (29) Henkelman, G.; Jónsson, H. Improved Tangent Estimate in the Nudged Elastic Band Method for Finding Minimum Energy Paths and Saddle Points. *J. Chem. Phys.* **2000**, *113*, 9978–9985.